A simulation-based approach for resilience assessment of process system
A case of LNG terminal system

Sun, Hao; Yang, Ming; Zio, Enrico; Li, Xinhong; Lin, Xiaofei; Huang, Xinjie; Wu, Qun

DOI
10.1016/j.ress.2024.110207

Publication date
2024

Document Version
Final published version

Published in
Reliability Engineering and System Safety

Reliability Engineering and System Safety 249 (2024) 110207

Contents lists available at ScienceDirect

Reliability Engineering and System Safety

journal homepage: www.elsevier.com/locate/ress

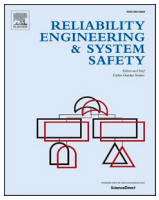

A simulation-based approach for resilience assessment of process system: A case of LNG terminal system

Hao Sun [a,b,*], Ming Yang [b,c], Enrico Zio [d,e], Xinhong Li [f], Xiaofei Lin [a], Xinjie Huang [a], Qun Wu [g,h]

[a] School of Civil Engineering and Architecture, Anhui University of Technology, Ma'anshan, Anhui 243002, China
[b] Safety and Security Science Section, Department of Values, Technology, and Innovation, Faculty of Technology, Policy, and Management, Delft University of Technology, the Netherlands
[c] Australian Maritime College, University of Tasmania, Launceston, TAS 7250, Australia
[d] MINES Paris-PSL University, France
[e] Energy Department, Politecnico di Milano, Italy
[f] School of Resources Engineering, Xi'an University of Architecture and Technology, No.13 Yanta Road, Xi'an 710055, China
[g] School of Mathematical Sciences, Anhui University, Hefei, Anhui 230601, China
[h] Anhui University Center for Applied Mathematics, Anhui University, Hefei, Anhui 230601, China

ARTICLE INFO

Keywords:
Resilience
Process safety
Dynamic simulation
LNG terminal system

ABSTRACT

System resilience denotes the capacity to uphold desired system performance in the face of disruptions. Evaluating the resilience of a process system necessitates a thorough consideration of the intricate interplay between its components and the pivotal role of process parameters in reflecting the repercussions of disruptions on the system. This paper introduces an integrated methodology that takes into account component interactions and leverages process data for the resilience assessment of a process system. The proposed methodology comprises four key components: system structure analysis, disruption impacts analysis, process simulation, and resilience assessment. Firstly, the system structure is meticulously scrutinized using a P-graph model. This analysis encompasses the assessment of the significance and interplay of components, as well as the evaluation of how component failures affect the system's overall processes. Secondly, a Markov model is devised to examine the state transition process of components and quantifies the maintenance time needed for failed components. Subsequently, a simulation model is formulated to acquire real-time process parameters in the presence of disruptive events. Finally, the system's performance response function (PRF) is derived from the normalization of these process parameters. Building upon this foundation, a resilience assessment is conducted with a focus on the PRF. To illustrate the effectiveness of this methodology, an LNG terminal system is employed as an exemplar.

1. Introduction

Process systems are significant in meeting human energy demand and promoting social development with various goods and services. In recent years, the complexity of process systems has increased, leading to the intricate coupling and interdependence of components and processes [1–3]. A complex system is defined as "a system for which tightly coupled interacting phenomena yield a collective behavior" [4,5]. Looking from the failure side, this means that when a component functionality is disrupted by external disruptions (e.g., environmental factors, intentional attacks, and human factors from outside the system) or internal disruptions (e.g., technical factors and random failures), the changing state of this component may impact on the functionality of other components of the system and the holistic process [6,7].

Unfortunately, recurring process safety accidents show that disruptions are difficult to avoid completely [8–10]. Once a system is affected by disruptive events, its performance decreases, impacting system productivity and safety. To maintain system performance under disruptive conditions, the concept of resilience has attracted extensive attention [11–16].

The term 'resilience' originated from the ecology field [17]. As a fundamental concept in Material Science, resilience is used to describe the ability of a material to bounce back to its initial state after deformation [18]. Then, resilience is regarded as an emergent property describing the ability of a system to maintain its performance under disruptive events [19–22]. Various definitions of resilience have been

* Corresponding author at: School of Civil Engineering and Architecture, Anhui University of Technology, Ma'anshan, Anhui 243002, China.
E-mail addresses: sunhao_upc@outlook.com, sunhao@ahut.edu.cn (H. Sun).

https://doi.org/10.1016/j.ress.2024.110207
Received 23 October 2023; Received in revised form 7 April 2024; Accepted 13 May 2024
Available online 21 May 2024

proposed. Haimes [23] defined resilience as the system's ability to resist a significant disruption within acceptable degradation parameters and recover within an acceptable time and composite costs and risks. Francis and Bekera [24] regarded resilience as the system ability concerning four tasks: absorption, adaptation, restoration, and learning. The American Society of Mechanical Engineers (ASME) views resilience as the system's ability to deal with external and internal disturbances without interrupting system functions. Hosseini et al. [13] surveyed papers published from 2000 to 2015. The results show that because different systems have different characteristics, there is no unified and standard concept of resilience. Cottam et al. [25] reviewed the engineered systems resilience literature from 1996 to 2018. They provided the following definition of system resilience: "successfully complete its planned mission(s) in the face of disruption(s) (environmental or adversarial), and has capabilities allowing it to complete future missions with evolving threats successfully".

Based on definitions of resilience, various resilience assessment methods have been developed according to system characteristics and resilience definition. Marino and Zio [11] proposed a generic framework and probabilistic methodology for resilience analysis of complex natural gas pipeline networks. The maximum gas supply capacity is regarded as the system performance indicator to assess the resilience of the system. Fang and Zio [26] developed an adaptive robust optimization-based framework for resilience assessment and improvement of interdependent critical infrastructure systems The probability of failure and recovery of system components is employed to analyze the impacts of a disruptions. Sun et al. [27] presented a DBN-based approach to assess safety barriers resilience for a process system. The system availability is considered a system performance indicator and used to assess the system resilience. An et al. [28] developed a comprehensive resilience assessment approach for an emergency response system. System-Theoretic Accident Model and Processes (STAMP) model is used to determine inappropriate control actions and develop dynamic Bayesian network (DBN) model. The system availability is regarded as the system performance indicator, which can be obtained from the DBN model. Kammouh et al. [29] introduced an indicator-based methodology to assess the resilience of engineering systems. Each indicator has different sub-indexed. Dynamic Bayesian network is utilized to describe the logic relationship between resilience, the indicators and the various sub-indexes. On the basis of that, the system resilience can be assessed. Tong and Gernay [22] proposed a probabilistic resilience assessment methodology for process industry facilities using DBN. The state of storage tanks is viewed as the system performance indicator, which can be quantified by DBN and probit model. The resilience of a storage tank farm is assessed based on the system performance. Cai et al. [30] introduced a DBN-based methodology to assess system resilience under different types of disruptions. The availability is defined as system performance indicator and estimated by a DBN model. Then, system resilience is obtained according to system performance. Zinetullina et al. [31] proposed an integrated resilience assessment approach for chemical process systems based on Functional Resonance Analysis Method (FRAM) and DBN. FRAM is used to identify the critical coupling of the system. DBN is used to quantify system performance and system resilience.

Although various resilience assessment approaches have been proposed, the intricate interaction and coupling relationships between system components are rarely considered. In addition, according to the above literature review, the resilience assessment is carried out by using availability/reliability-based performance indicator. However, the source of reliability data is uncertain. For example, the data comes from a reliability history database or expert opinion. Although a variety of methods to deal with data uncertainty have been proposed, the influence of uncertainty on results cannot be completely eliminated. Besides, the process parameters of process systems have multi-dimensional characteristics, and the process parameters change complicated after being affected by disruptions. Reliability/availability cannot accurately quantify and express the complex dynamic response mechanism of various parameters under the influence of disruptive events.

Towards this end, to surmount the deficiency of existing methods, we introduce a process parameters-based performance indicator to conduct resilience assessment of process systems from techno-centric perspective. Compare to availability/reliability-based performance indicator, it has three advantages: (1) it can be obtained from the time-dependent data of the system, which means that the impact of data uncertainty can be largely avoided; (2) the process parameters are able to intuitively reflect the impact of disruptive events on system performance. (3) resilience refers not only to the system's ability to maintain operational functionality in the face of disruptions (a perspective closely associated with reliability) but also encompasses the system's capacity to adapt and recover from such events, restoring its original state or evolving into a new, more robust state.

The proposed methodology aims to assess the resilience of a process system considering components interactions and the impact of disruptions directly on the system process parameters. Firstly, a P-graph model is developed to describe the interactions between components and qualitatively evaluate the impact of component failure caused by disruptions. Then, a Markov process model is introduced for reflecting the state transition process of components and quantify the required maintenance time for those affected by disruption. Thirdly, a process simulation model is constructed and run to obtain the process parameters of the system during the absorption, adaptation, and restoration phases under a disruption. By normalization of the system time-dependent process parameters, the system performance response function (PRF) is obtained. Finally, a resilience metric is proposed to assess the resilience of the process system based on PRF.

The main contributions of the study are:

(1) The interactions between components are analyzed by using a P-graph model, which offers an effective way to represent the impact of a component failure on the system process and to qualitatively determine the importance of each component.
(2) To avoid the impact of data uncertainty and directly reflect the impact of disruptions on the system performance, a process parameters-based indicator is proposed to represent system performance based on time-dependent system process data.
(3) Different combinations of system performance response function and recovery time may give a similar resilience value [32]. We propose a procedure to compare system resilience.

The remainder of the paper is organized as follows. The proposed resilience assessment methodology, including the P-graph model, simulation model and the resilience metric, is presented in Section 2. A case study is conducted in Section 3, Finally, Section 4 concludes the paper.

2. The proposed methodology

Fig. 1 presents the framework of the proposed methodology, which mainly includes four steps, as follows.

Step I: System structure analysis. The P-graph method is used to identify interactions of components and analyze the system structure according to the process flow of the system. Then, the functions and redundancy settings of each component are determined. Subsequently, the impact on the system of the failure of each component is analyzed to qualitatively determine the importance of each component. The more important a component is, the greater the impact on the system if it fails. On this basis, the results of system structure analysis can be used to help operators identify potential disruptive events.

Step II: Disruption impacts analysis. According to the qualitative importance analysis in step I, the impacts of potential disruptions are assessed. A Markov model is employed to represent the degradation and maintenance processes, and the maintenance time required by a

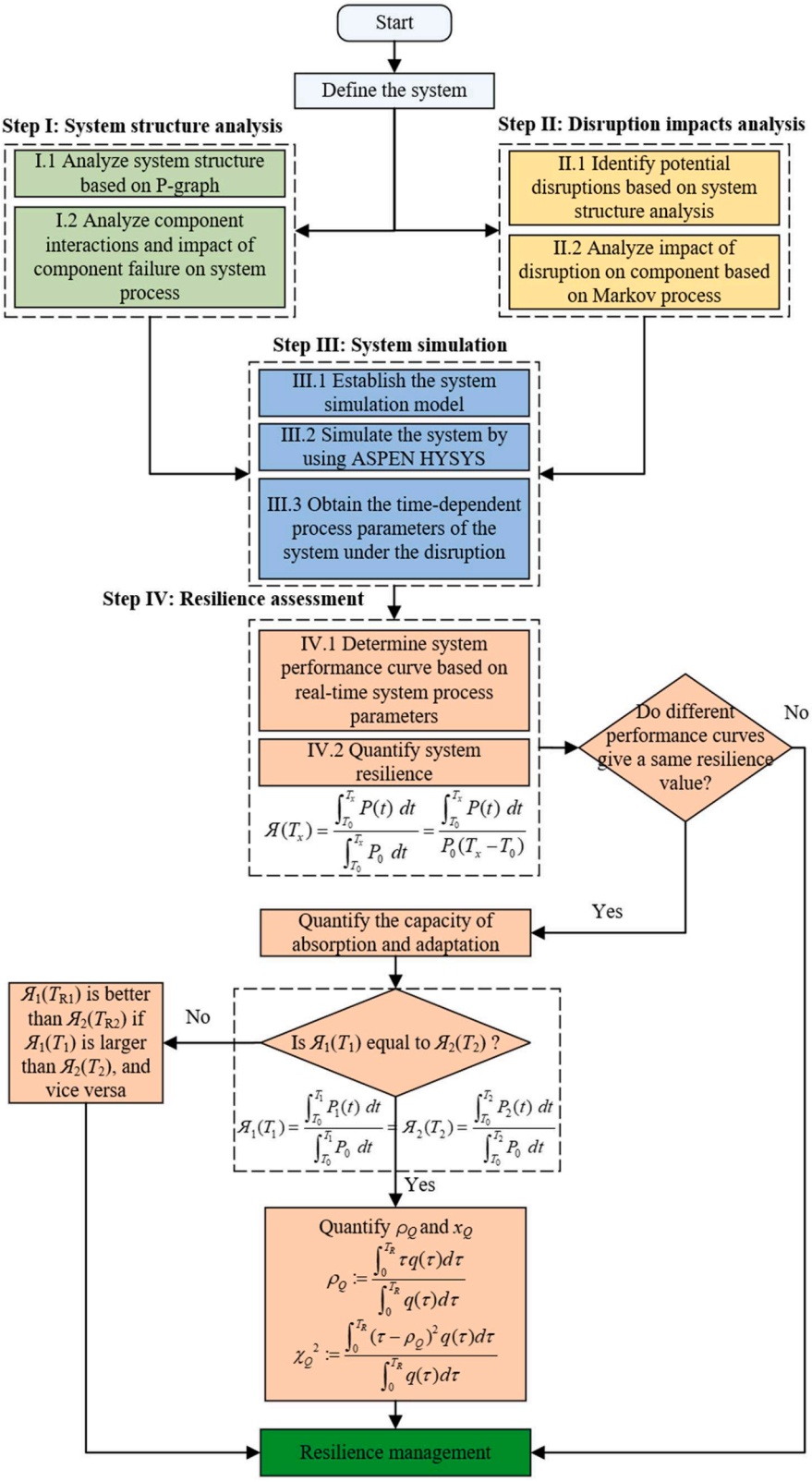

Fig. 1. The proposed methodology for assessing the system resilience.

component after disruptions is computed.

Step III: Process simulation using HYSYS. The maintenance time after component failure obtained from Step II is used as the input of process simulation, and the time-dependent parameters of the system during this period and its change over time are obtained and analyzed by the process simulation software. In this paper, the process simulation software, HYSYS, is employed to obtain time-dependent process data under disruptive events.

Step IV: Resilience assessment. The system PRF can be generated by normalizing time-dependent process data obtained from Step III.

Based on the PRF, we propose a novel resilience assessment methodology to assess and manage system resilience. Subsequently, the targeted measurements of improving system resilience are developed.

2.1. System structure analysis based on P-graph method

Analyzing the structure of a process system and identifying the important component play a key role in resilience assessment and management. The P-graph method is an effective way to analyze the structure of process systems [33]. According to process flow diagram (PFD), it enables to present complex production processes and the redundancy settings of the various system components in the form of network diagrams. In other words, P-graph is the simplified version of PFD. Compared with PFD, it can intuitively present the relationship between the various components of the system and the redundancy situation, which is convenient to analyze the interactions of system components and impact of disruptions on the system process.

P-graph consists of four main elements: raw material nod, operation unit node, production node, and material transfer arc. An example of the P-graph method is shown in Fig. 2. As can be seen from Fig. 2, two streams of raw materials F1 and F2 enter components C1 and C7 respectively. F1 is transported to components C2, C3, C5 and C6 after being processed by component C1, and then mixed with materials of component C9. Finally, production M is produced after being processed by C9. The solid black line in Fig. 2 shows the production process under normal operating conditions of the system. The black dotted line indicates the working flow of redundant devices. When C3, C7, and C9 are malfunctioning, the corresponding redundant device is activated to ensure the normal operation of the system. However, when a non-redundant design device fails (such as C1), it can interrupt the production process of the system and affect the delivery of production M. The P-graph method can be employed to express the structure of a complex system in an intuitive way and analyze the complex interactions between components and display the redundancy settings of each component in the system. On this basis, the importance of component and potential disruptive events can be determined.

2.2. Disruption impacts analysis based on Markov process modelling

Let $Y(t)$ be a random process with a set of performance states $S=\{S_0, S_1, \ldots, S_k\}$. S_0 represents the highest performance state of the system and S_k refers to the lowest performance state of the system. Assume the system performance state at time t is $Y(t)=i$; then, the probability that system performance state is j at time $t+1$ is:

$$P\{Y(t+1)=j|Y(t),Y(t-1),\cdots,Y(t_2),Y(t_1)\} \tag{1}$$

As well known, if Eq. (1) satisfies Eq. (2), then the process is regarded as a Markov process. The future state of a random process with Markov properties is only related to its current state and not to the past state:

$$P\{Y(t+1)=j|Y(t),Y(t-1),\cdots,Y(t_2),Y(t_1)\}=P\{Y(t+1)=j|Y(t)=i\} \tag{2}$$

The system state changes following disruptive events and maintenance activities. If the system is affected by disruptions, the system state may degrade from S_i to S_j with rate $\lambda_{i,j}$. The maintenance activities are conducted when the system performance state transfers to failure state [34]. When the system is repaired, the state of the system may jump back from S_j to S_i with rate $\mu_{j,i}$. The state transition rate matrix A of the system can be expressed as Eq. (3):

$$A=\begin{bmatrix} q_{1,1}q_{1,2}\cdots q_{1,k} \\ q_{2,1}q_{2,2}\cdots q_{2,k} \\ \vdots\vdots\ddots\vdots \\ q_{k,1}q_{k,2}\cdots q_{k,k} \end{bmatrix} \tag{3}$$

The state transition probability matrix $P(t)$ of the system is as Eq. (4):

$$P(t)=\begin{bmatrix} P_{1,1}(t)P_{1,2}(t)\cdots P_{1,k}(t) \\ P_{2,1}(t)P_{2,v2}(t)\cdots P_{2,k}(t) \\ \vdots\vdots\ddots\vdots \\ P_{k,1}(t)P_{k,2}(t)\cdots P_{k,k}(t) \end{bmatrix} \tag{4}$$

$$q_{ij}=\begin{cases} \lambda_{i,j}, i<j \\ -\left(\sum_{j=0}^{i-1}\mu_{i,j}+\sum_{j=i+1}^{k}\lambda_{i,j}\right), i=j \\ \mu_{i,j}, i>j \end{cases} \tag{5}$$

where, $q_{i,j}$ represents the transition rate from state S_i to state S_j, which is determined by failure rate λ and repair rate μ. $P_{i,j}$ represents the transition probability from state S_i to state S_j and $P_{i,i}(t)=1-\sum_{j=0,j\neq i}^{k}P_{i,j}(t)$, $q_{i,i}=\frac{\partial P_{i,i}(t)}{\partial t}$ and $q_{i,j}=\frac{\partial P_{i,j}(t)}{\partial t}$ [35].

Taking a component with four states as an example, as shown in Fig. 3. According to Eqs. (3) and (5), the state transition rate matrix of the component can be expressed as:

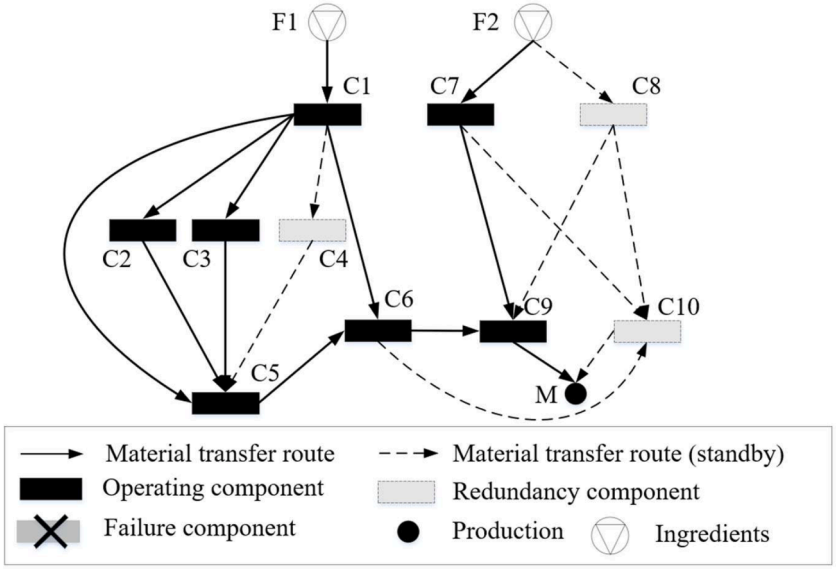

Fig. 2. Illustrative example of a P-graph.

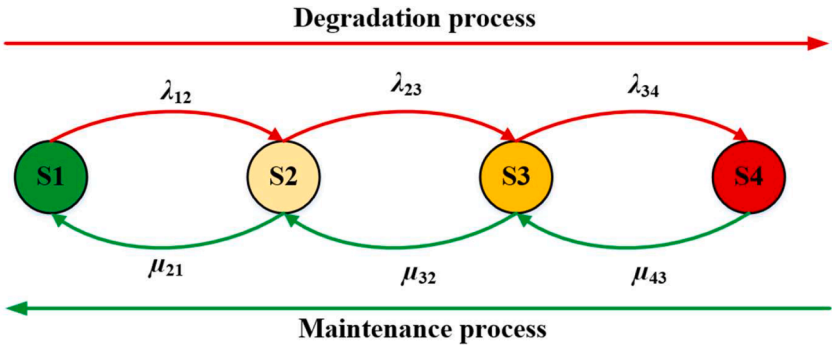

Fig. 3. The illustrative example of Markov model.

$$A = \begin{bmatrix} q_{1,1}q_{1,2}q_{1,3}q_{1,4} \\ q_{2,1}q_{2,2}q_{2,3}q_{2,4} \\ q_{3,1}q_{3,2}q_{3,3}q_{3,4} \\ q_{4,1}q_{4,2}q_{4,3}q_{4,4} \end{bmatrix} = \begin{bmatrix} -\lambda_{1,2}\lambda_{1,2}00 \\ \mu_{2,1} - \mu_{2,1} - \lambda_{2,3}\lambda_{2,3}0 \\ 0\mu_{3,2} - \mu_{3,2} - \lambda_{3,4}\lambda_{3,4} \\ 00\mu_{4,3} - \mu_{4,3} \end{bmatrix} \tag{6}$$

2.3. Process simulation

The structure of process systems is complex. In addition, a large number of dangerous substances are involved in the process of production, processing and storage. The physical experiment to explore the impact of disruptions on process system is accompanied by great risks and costs. Based on the process flow, the process simulation software can be used to "reproduce" the process system by compiling the physical parameters, state functions, differential and integral functions of the whole process flow through computer language [36]. In particular, Aspen HYSYS is widely used in petrochemical, biopharmaceutical and energy fields [37,38].

Real-time values of the system process parameters (e.g., pressure, temperature, liquid level, and etc.) under disruptive events can be obtained from HYSYS simulations. Since the performance of the process system is represented by the system process parameters, it is necessary to normalize the real-time data to determine system performance curve. According to the expected value, actual value and upper and lower limit values of the system performance indicator, the real-time data is processed by Eq. (7) when P_{rt} is greater than P^*. Otherwise, the real-time data is processed by Eq. (8) when P_{rt} is less than P^*. The normalized data is the real-time performance data of the system, and the performance range is [0, 1]. 0 indicates that the system is in the failure state, and 1 represents that the system is in the highest performance state.

$$\psi(t) = 1 - \frac{P_{rt} - P^*}{P_{Max} - P^*} \tag{7}$$

$$\psi(t) = 1 - \frac{P^* - P_{rt}}{P^* - P_{Min}} \tag{8}$$

whereψrefers to system performance after normalization, P_{rt} is the measured value of the system parameters; P^* is the expected value for normal working conditions; P_{Max} is the maximum acceptable upper limit, beyond which serious safety or production problems can be caused; P_{Min} is the minimum acceptable lower limit.

2.4. Resilience assessment

As explained in the previous section, the system performance curve (Fig. 4), can be obtained from process simulation and normalization. In some studies, resilience is indicated by the ratio of the area under the performance curve $P(t)$ to the area under the initial performance curve from T_0 (disruption occurrence time) to T_R (time to recovery to a new equilibrium state) [15,27,39,40].

Accordingly, the instantaneous resilience can be expressed as:

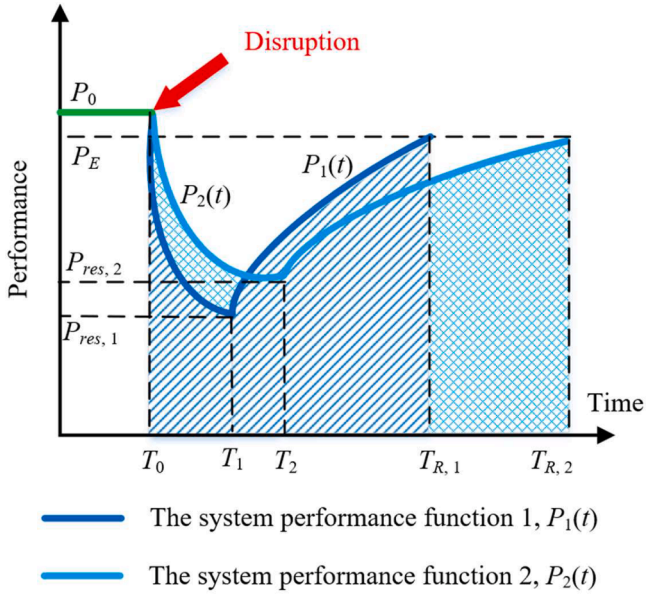

Fig. 4. The two different system performance curves.

$$\mathcal{R}(t|e^j) = \frac{\Phi(t|e^l) - \Phi(t_d|e^l)}{\Phi(t_0) - \Phi(t_d|e^l)} \tag{9}$$

where $\mathcal{R}(t|e^j)$ indicates system resilience at time t; $\Phi(t|e^l)$ represents system performance at time t; $\Phi(t_d|e^l)$ is the lowest performance of the system; $\Phi(t_0)$ indicates the initial performance of the system before the occurrence of the disruption. Eq. (9) can be changed to Eq. (10) by integrating over time:

$$\mathcal{R}(T_x) = \frac{\int_{T_0}^{T_x} P(t)dt}{\int_{T_0}^{T_x} P_0 dt} = \frac{\int_{T_0}^{T_x} P(t)dt}{P_0(T_x - T_0)} \tag{10}$$

where $\mathcal{R}(T_x)$ refers to the resilience of the system over the considered time position; P_0 indicates the system initial performance before disruptions occur; P_E indicates a new equilibrium performance of the system; T_x is the time between T_0 and T_R ($T_0 < T_x < T_R$); T_0 represents the occurrence time of the disruption.

Clearly, different combinations of $P(t)$ and T_R may lead to the same resilience value $\mathcal{R}(T_R)$ [32], although with different characteristics of system resilience. To address this issue, we propose a resilience comparison procedure, which can be seen Step IV in Fig. 1. Resilience consists of three primary capacities: absorption, adaptation and restoration [41,42]:

- Absorption is the intrinsic ability of the system to resist damage of disruptions. The absorption capacity is dependent on system structure. It can absorb effects of disruptions on system and mitigate the consequences. High absorption capacity can reduce the probability of system failure and mitigate system performance loss. The stronger the absorption capacity of the system, the less the system is affected by disruptions.
- Adaptation is the ability of a system to adapt to disruptions. High adaptation capacity indicates a higher level of performance after disruption.
- Restoration capacity refers to the ability of a system to restore its performance to a new equilibrium state after being affected by disruptions. It is dependent on external maintenance resources.

It can be seen from descriptions of three different capacities, absorption and adaptation capacity depend on system structure and organization ([43]; Sun et al., 2022). If the system has a strong absorption and adaptation capacity, it can reduce the impact of disruptions on the system performance and reduce the dependence of the system on the restoration capacity. Absorption and adaptation belong to the intrinsic capacities of the system. On the contrary, restoration capacity depends on external maintenance resources. From the perspective of intrinsic safety, the absorption and adaptation capacity are given higher priority than the recovery capacity.

When different combinations of $P(t)$ and T_R lead to simialr resilience values $\mathcal{R}(T_R)$, absorption and adaptation capacity can be used to differentiate system resilience. Take system performance curve $P_1(t)$ and $P_2(t)$ of Fig. 4 as an example. For $P_1(t)$, the disruption occurrence time is T_0; the process of absorption and adaptation is from T_0 and T_1; the restoration period is between T_1 and $T_{R,1}$; the absorption and adaptation capacity $\mathcal{R}(T_1)$ can be represented by the ratio of the area under the performance curve $P_1(t)$ to the area under the initial performance curve from T_0 to T_1. For $P_2(t)$, the disruption occurrence time is T_0; the process of absorption and adaptation is from T_0 and T_2; the restoration process is between T_2 and $T_{R,2}$; the absorption and adaptation capacity $\mathcal{R}(T_2)$ can be represented by the ratio of the area under the performance curve $P_2(t)$ to the area under the initial performance curve from T_0 to T_2. Therefore, when different combinations of $P(t)$ and T_R have a same resilience value $\mathcal{R}(T_R)$, the resilience of the system can be differentiated by comparing the values of $\mathcal{R}(T_1)$ and $\mathcal{R}(T_2)$:

$$\mathcal{R}(T_1) = \frac{\int_{T_0}^{T_1} P_1(t)dt}{\int_{T_0}^{T_1} P_0 dt} \tag{11}$$

$$\mathcal{R}(T_2) = \frac{\int_{T_0}^{T_2} P_2(t)dt}{\int_{T_0}^{T_2} P_0 dt} \tag{12}$$

When $\mathcal{R}(T_1)$ is greater than $\mathcal{R}(T_2)$, it means that $P_1(t)$ is better than $P_2(t)$ in the view of intrinsic safety, and vice versa. However, there are also cases in which $\mathcal{R}(T_1)$ equals $\mathcal{R}(T_2)$. In this situation, restoration capacity is compared to differentiate the system resilience. For this, Sharma et al. (2020) proposed Center of Resilience and Resilience Bandwidth based on probability theory and mechanics. The recovery curve $Q(\tau)$ is defined as *Cumulative Resilience Function* (CRF). When the CRF is a continuous function of time, the Instantaneous Rate of the Recovery Progress (IRRP) can be obtained by the time derivative of the CRF. IRRP is regarded as $q(\tau)=dQ/d\tau$ for all $\tau\in[0, T_R]$, which is called *Resilience Density Function* (RDF). T_R indicates the whole recovery time. Then, the recovery process over any time interval $(\tau_u, \tau_v] \subseteq [0, T_R]$ is shown in Eq. (13). When the CRF is a step function or a combination of continuous function and step function of time, the recovery process over any time interval can be seen as:

$$Q(\tau_u < \tau < \tau_v) = \int_{\tau_u}^{\tau_v} q(\tau)d\tau \tag{13}$$

The Center of Resilience ρ_Q, which combines residual performance and recovery time, is defined as:

$$\rho_Q := \frac{\int_0^{T_R} \tau q(\tau)d\tau}{\int_0^{T_R} q(\tau)d\tau} = \frac{Q_{res}}{Q_{tar}}\rho_{Q,res} + \frac{Q_{res1}}{Q_{tar}}\rho_{Q,res1} \tag{14}$$

where Q_{res} represents the residual performance of system, Q_{tar} equals to $Q(T_R)$, $\rho_{Q,res}=\tau_0$, $Q_{res1}= Q_{tar} - Q_{res}$. Due to $\tau_0 = 0$, Eq. (14) can be converted into Eq. (15):

$$\rho_Q = \frac{Q_{res1}}{Q_{tar}}\rho_{Q,res1} \tag{15}$$

The Resilience Bandwidth χ_Q, as a measure of dispersion of recovery, is defined as:

$$\chi_Q{}^2 := \frac{\int_0^{T_R} (\tau - \rho_Q)^2 q(\tau)d\tau}{\int_0^{T_R} q(\tau)d\tau} \tag{16}$$

A small value of χ_Q means that the recovery process is finished during a short period around ρ_Q; on the contrary, a large value indicates that the recovery process is spread over a long time. Once the system functionality curve is obtained, the ρ_Q and χ_Q can be determined based on Eqs. (15) and (16).

3. Case study

Due to its easy storage and transportation, large gas-liquid expansion ratio and high energy efficiency, Liquefied Natural Gas (LNG) is known as the cleanest fossil energy on Earth [44,45]. The LNG terminal system comprises four key components: the unloading system, storage system, Boil Off Gas (BOG) treatment system and gasification system. The role of the unloading system is to transfer the LNG on board to the storage tank through the unloading arms. To manage BOG and prevent overpressure in the storage tank, the BOG treatment system comes into play. Its primary role involves compressing BOG and harnesses the cold energy of LNG to condense BOG back into LNG, minimizing production losses. The recondensed LNG, along with the LNG in the storage tank, is then transported to the LNG gasification system to transform the LNG into natural gas. This conversion serves to meet the energy requirements of downstream users [46].

3.1. System structure analysis

Taking the LNG terminal system as an example, the P-graph method is utilized to analyze the structure of the system, as shown in Fig. 5. The material F1 (LNG) enters the storage tank C1, and the BOG generated in C1 is compressed by the compressor C2 and C3 (C4 is the standby compressor) and then transported to the condenser C5. The cold energy of LNG is utilized to reliquefy the compressed BOG into LNG in C5. The liquefied LNG and the LNG in C1 are transported to the vaporizer C11 (C12 is the standby vaporizer) through high pressure pump C6 (C7 is the standby pump). After heat exchange in the vaporizer C11 with seawater transported by sea water pumps C8 and C9 (C10 is the standby sea water pump), the low-temperature LNG is changed into product M (natural gas), thus meeting the energy needs of downstream users. The P-graph analysis process is shown in Fig. 5, and the meanings of symbols in Fig. 5 are shown in Table 1.

Fig. 5 shows the system production process and the redundancy of each component. According to the production process, composition and redundancy of each component of the LNG terminal system, the influence of each component failure on the system is analyzed. When C1 fails, the whole process will be terminated, as shown in Fig. 6. With no source

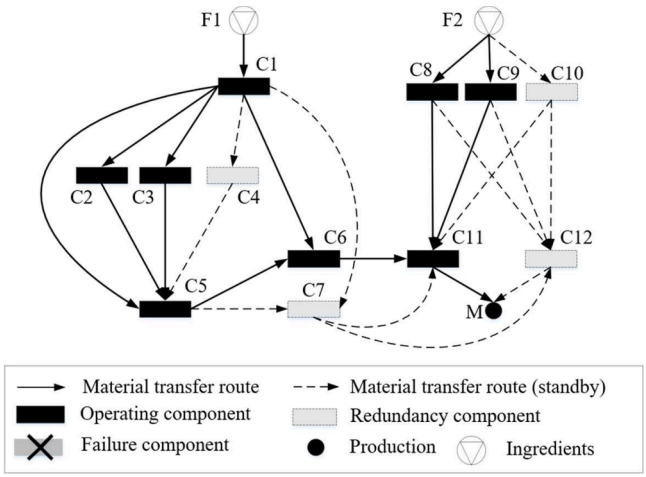

Fig. 5. Structure analysis of LNG terminal system based on P-graph method.

Table 1
Meaning of the symbols in the LNG terminal system structure analysis diagram.

Symbols	Description	Symbols	Description
F1	LNG	C6, C7	High pressure pumps
F2	Sea water	C8, C9, C10	Sea water pumps
C1	LNG tank	C11, C12	Vaporizers
C2, C3, C4	Compressors	M	Natural gas
C5	Condenser	—	—

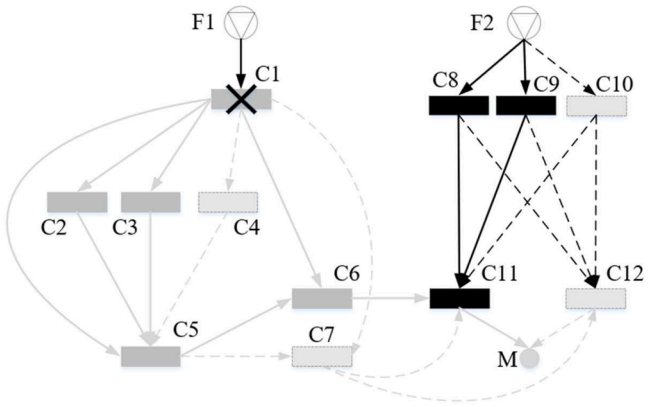

Fig. 6. Structure analysis of the system in the case C1 fails.

of feedstock, the entire LNG processing and transportation process is terminated, and the product M cannot be generated. Therefore, ensuring the safety of LNG storage tanks is the basis for ensuring the safe production of LNG terminal systems. The high pressure, low pressure and high liquid level inside the LNG tank of the LNG terminal are the main causes of the LNG storage tank accidents, and the consequences of the accidents are severe. Therefore, when analyzing the LNG terminal system, the change of physical parameters such as the pressure and liquid level in the LNG tank with time should be considered.

To deal with the BOG in the LNG tank, there are three compressors in the compressor system. The number of working compressors is determined by the LNG tank pressure during normal operation. If the tank pressure rise caused by BOG is under normal level, only one compressor C2 is needed. If the tank pressure rise due to BOG is too large, the two compressors C2 and C3 should be activated at the same time to ensure the efficiency of handling BOG. C4 is the backup compressor in case of the simultaneous failure of C2 and C3. BOG is discharged through flare system or safety valve when the whole compressor system fails. The startup and shutdown of the compressor are controlled by the pressure controller according to the pressure inside the tank. Compressor failure scenarios can be divided into three categories: compressor C2 fails, compressor C2 and C3 fail, and compressor C2, C3 and standby compressor C4 fail simultaneous. The system structure analysis of three different scenarios is shown in Fig. 7.

We also analyze the impact of other component fault (e.g., high-pressure pump fault and sea water pump) on the system process. The results show that those scenarios can cause production disruptions, but they do not lead to serious accidents.

From the above analysis, it can be seen that LNG tank is the pivot of the entire production process. If an LNG storage tank accident occurs, it will not only interrupt the production but also cause serious casualties, property losses and environmental damage. Therefore, it is critical to ensure the safety of LNG tanks. Since compressor failure may lead to tank overpressure accidents, compressor failure is regarded as the disruptive event for the LNG terminal system, and the resilience of the LNG terminal system under different failure combinations is evaluated.

3.2. Disruption impacts analysis

The P-graph method is used to analyze the system structure, interactions between components, and determine the potential disruption (i.e., compressors fail). On this basis, the Markov model is established to analyze and quantify the state transition and required maintenance time after the disruptive events. After that, the time required for the compressors to return to normal operation can be obtained. The time is taken as the time point to restart the compressors.

The Markov model of the compressor state transition is shown in Fig. 8. The compressor has four states: S indicates that the device is in a safe state; $D1$ and $D2$ represent the intermediate states of the degradation process. The state of $D2$ is worse than that of $D1$, but the compressor can still run when it is in the $D1$ and $D2$ states. F refers to fault state, which means that the compressor cannot run properly. The transition process between the various states of the compressor is determined by the failure rate λ and the repair rate μ, as shown in Fig. 8. It is assumed that failure rate λ and repair rate μ follow exponential distributions [30,47].

According to Eqs. (5) and (6), the state transition rate matrix A of compressor can be depicted as:

$$A = \begin{bmatrix} q_{S,S}q_{S,D1}q_{S,D2}q_{S,F} \\ q_{D1,S}q_{D1,D1}q_{D1,D2}q_{D1,F} \\ q_{D2,S}q_{D2,D1}q_{D2,D2}q_{D2,F} \\ q_{F,S}q_{F,D1}q_{F,D2}q_{F,F} \end{bmatrix} \tag{17}$$

$$A = \begin{bmatrix} -(\lambda_1+\lambda_4+\lambda_5)\lambda_4\lambda_5\lambda_1 \\ \mu_4-(\lambda_2+\lambda_6+\mu_4)\lambda_6\lambda_2 \\ \mu_5\mu_6-(\lambda_3+\lambda_5+\mu_6)\lambda_3 \\ \mu_1\mu_2\mu_3-(\mu_1+\mu_2+\mu_3) \end{bmatrix} \tag{18}$$

The disruptive event of the system is the compressor failure. After compressor failure, a certain response time is required, that is, the time required for resource allocation. When all the preparatory work is completed, maintenance activities are conducted to repair the malfunctioning compressor. The time required for the compressor to recover from the failure state F to the safe state S is determined by the Markov process model. The repair rate of the compressor can be derived from OREDA database and related literature [48,49]. According to the relevant data, the repair rate μ of the compressor is 0.076/h. Because the failure rate λ and repair rate μ follow exponential distributions [30], the time required to repair the malfunctioning compressor to a safe state can be depicted as Eq. (19):

$$t = -\frac{\ln(1-P_{FS})}{\mu} \tag{19}$$

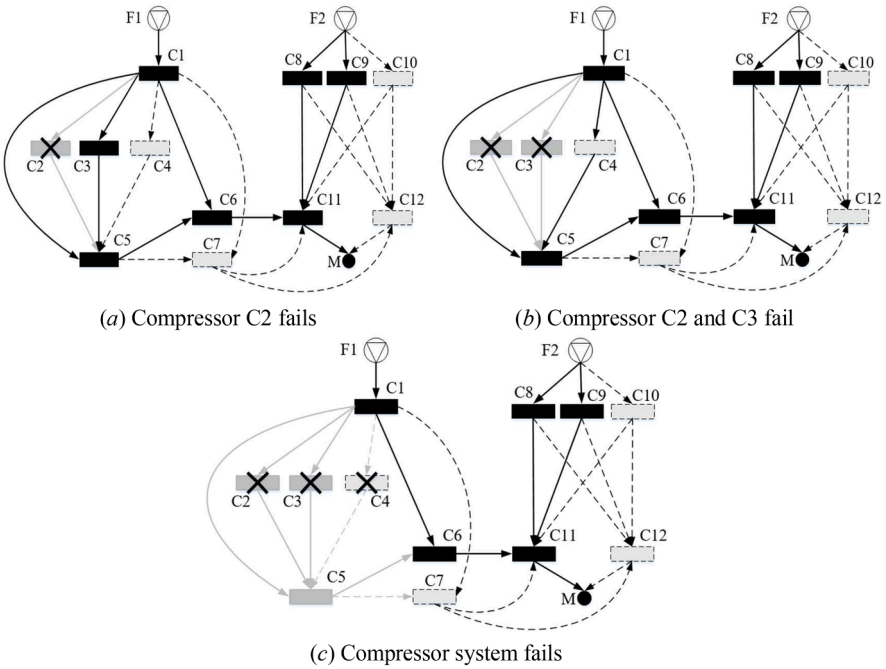

Fig. 7. Structure analysis of different compressor fails.

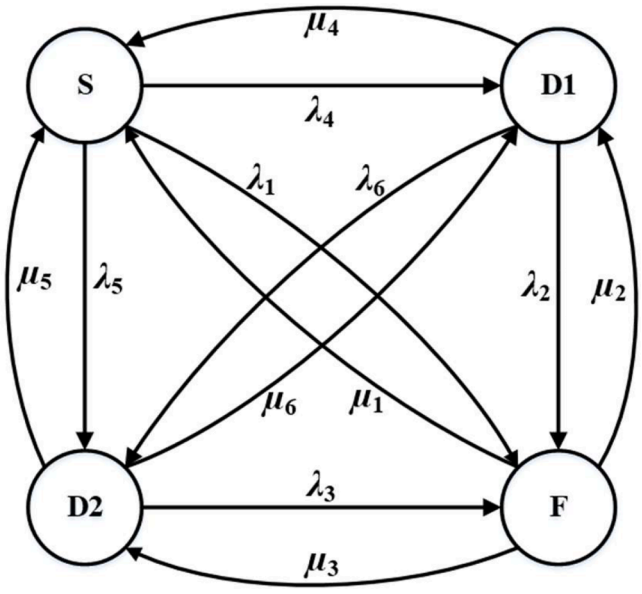

Fig. 8. The Markov model for the compressor state transition process.

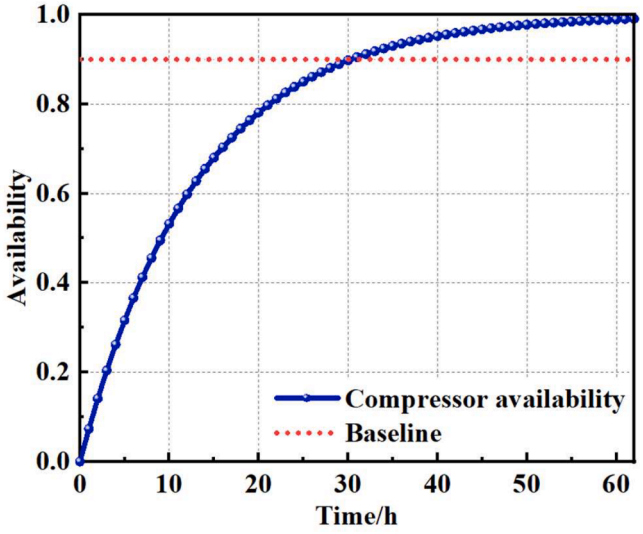

Fig. 9. Schematic diagram of maintenance time and availability of compressor.

where the P_{FS} indicates the probability of transition of from state F to S.

The results show that it takes 30.30 h to repair the compressor from the failure state F back to the safe state S. The compressor availability to recover from the failure state F to the safe state S over time is shown in Fig. 9. After the maintenance time is determined, the maintenance time is used as the restart time of the compressor in the process simulation to investigate the impact of disruptive events on the performance of the LNG terminal system and to quantify the system resilience.

3.3. System simulations

On the basis of determining the system parameters, the LNG terminal system simulation model is established by using the process simulation software ASPEN HYSYS, as shown in Fig. 10. The main input data, detailed settings and LNG compositions information are shown in Tables 2 and 3. According to the analysis in Section 3.1, compressor failure will lead to the accumulation of BOG in the LNG tank and the rise of pressure in the LNG tank, thus affecting the system safety. Therefore, the pressure in the LNG tank is selected as the safety performance indicator of the system. On this basis, the proposed resilience assessment method is applied to quantify the resilience of the LNG terminal system.

Without loss of generality, assume that the required response time of the system is 4 h, to complete task of the fault detection, disruption investigation and solution development and maintenance resources allocation. Due to the required maintenance time is 30.30 h, and thus the total time from the failure to the maintenance of the compressor to the safe state is 34.30 h. Compressor failure scenarios consist of three different types according to different failure combinations (i.e., scenario 1: minor disruption, compressor C2 failure; scenario 2: moderate disruption, simultaneous failure of C2 and C3; scenario 3: severe

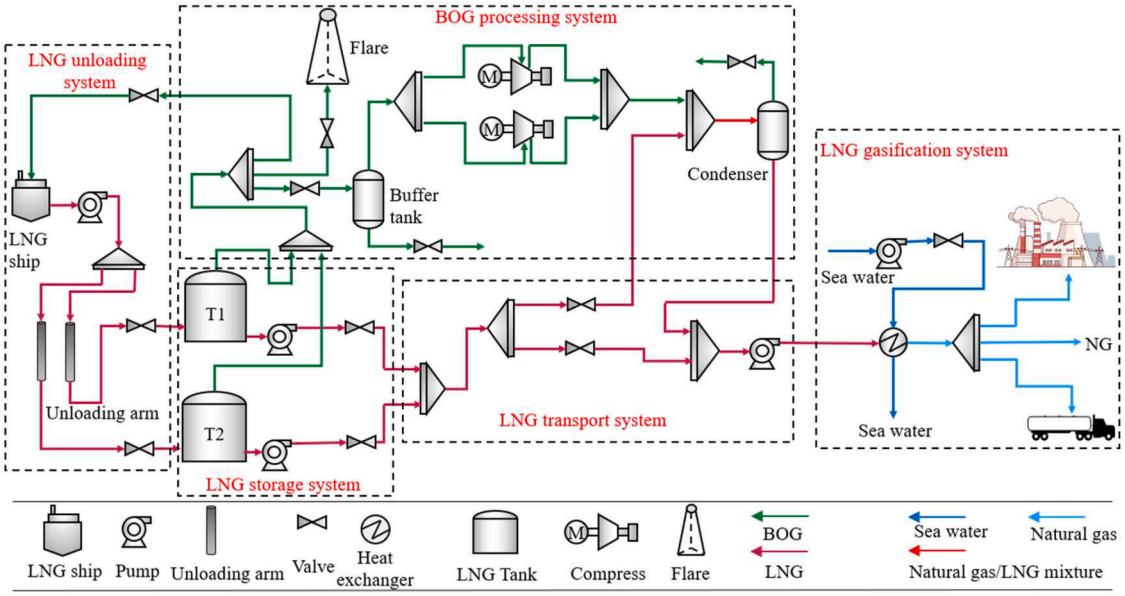

Fig. 10. The simulation model of the LNG terminal system.

Table 2
Main operation parameters of LNG terminal system.

Parameters	Temperature/ °C	Pressure/ kPa	Flow rate/ ($kg \cdot h^{-1}$)
Input of LNG tank	−161	116	1.07×10^6
Output of LNG tank	−158.5	116	1.046×10^6
Output of BOG	−158.5	116	2.4×10^4
Input of compressor	−158.5	116	1.2×10^4
Output of compressor	−70.73	700	1.2×10^4
Input of low-pressure pump	−158.5	116	1.046×10^6
Output of low-pressure pump	−158.5	800	1.046×10^6
Input of high-pressure pump	−153.4	600	1.069×10^6
Output of high-pressure pump	−149.4	7800	1.069×10^6

disruption, compressor system failure). Different scenarios have different disruption intensity and different impacts on system performance.

For the compressor failure scenario, the internal pressure of LNG tank is regarded as the performance indicator of the system, and the real-time data of LNG tank pressure under the disruptive condition is obtained by the process simulation software. The upper limit of the operating pressure of the LNG tank is 126 kPa, thus 126 kPa is viewed as the maximum acceptable pressure of the tank. Assuming that the disruptive event occurs at time 0. When the compressor C2 fails and the compressor C2 and C3 fail simultaneously, the tank pressure changes with time are shown in Fig. 11.

As can be seen from Fig. 11, when compressor C2 fails (scenario 1), the pressure inside the tank will not be affected by this disruption due to the presence of backup compressor C4. However, when C2 and C3 fail at the same time (scenario 2), only C4 can process the BOG generated in the tank, and the processing capacity is greatly affected. The BOG that is not processed in time exists in the tank, resulting in the tank pressure rising over time. At the 34.30 h when the compressor recovery to work is completed, the maximum tank pressure caused by the compressor failure is 122.57 kPa, which is lower than the maximum operating pressure of 126 kPa, as shown in Fig. 11. According to the simulation results, it takes 60.70 h for the tank pressure to recover to the initial value. Therefore, the total time required for the tank pressure to recover to the original value due to the disruptive event (scenario 2) is 95 h. The changes of the pressure in the tank during the whole process are shown in Fig. 11(*a*). Eq. (7) is applied to normalize the real-time data of tank pressure. The normalized data is used to generate the system performance curve, which can be seen in Fig. 11(*b*).

For a compressor system failure (Scenario 3), the tank pressure changes over time are shown in Fig. 12(*a*). As can be seen from the Figure, since the BOG generated in the LNG tank could not be processed in time, the tank pressure increases dramatically over time, and reaches the maximum operation pressure 126 kPa at 24.17 h. The maintenance time required for the compressor is 30.30 h, which is longer than the time required for the tank pressure to reach the maximum acceptable pressure of 126 kPa. If the flare system and safety valve fail in this scenario, the pressure of the tank will reach the maximum design pressure of the tank 130 kPa at the 35th hour. Under this scenario, the pressure in the tank will rise rapidly, and the failure of the compressor system will lead to the overpressure accident of the LNG tank. The system performance over time is shown in Fig. 12(*b*).

3.4. Quantification of the system resilience

(1) System resilience assessment under different disruptive events

According to the established resilience assessment method of process system, the system resilience under three different scenarios is evaluated based on the obtained system performance curve. Since the system takes different lengths of time to recover to the safe state under the three various scenarios, it is necessary to calculate and compare the system resilience under different scenarios.

Table 3
LNG compositions information.

Compositions	Methane	Ethane	Propane	Normal butane	Isobutane	Pentane and others	Nitrogen
Molar percentage (Mol%)	89.39	5.76	3.3	0.66	0.78	0.00	0.11

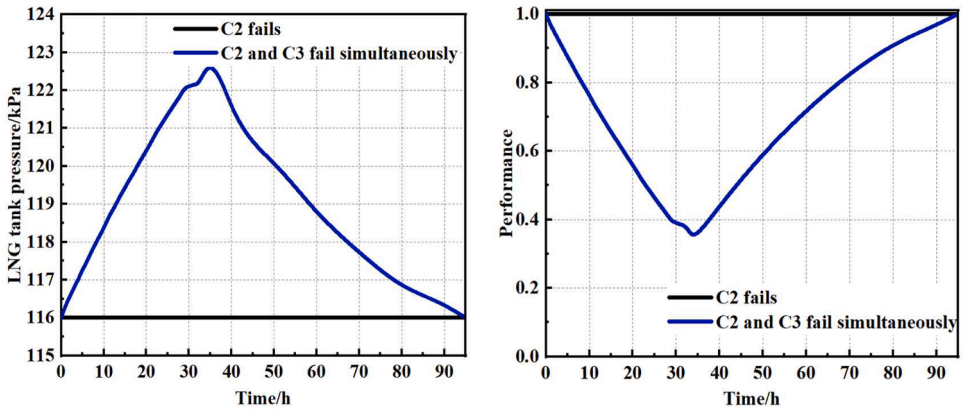

(*a*) Tank pressure over time (*b*) System performance over time

Fig. 11. Tank pressure (a) and performance (b) change with time in scenario 2.

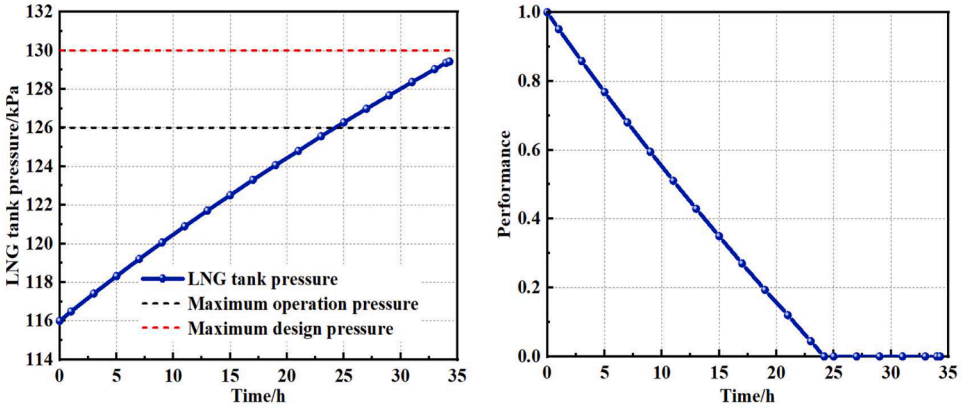

(*a*) Tank pressure over time (*b*) System performance over time

Fig. 12. Real-time values of the tank pressure (a) and system performance curve (b) after compressor system failure.

Scenario 1: Minor disruption (compressor C2 failure). In this scenario, the system performance curve is shown in Fig. 11(*b*), and the expression of the performance response curve $P_1(t)$ is shown in Eq. (20). On this basis, Eq. (10) is used to calculate the system resilience under this scenario. Since the performance of the system did not change after C2 failure, the system resilience is 1, as shown in Fig. 13:

$$P_1(t) = 1, 0 \le t \le 34.3\text{h} \tag{20}$$

Scenario 2: Moderate disruption (simultaneous failure of compressors C2 and C3). Fig. 11(*b*) shows the system performance curve when C2 and C3 are faulty at the same time. When C2 and C3 fail simultaneously, the backup compressor C4 is activated to deal with the BOG in the tank. In this situation, however, the processing efficiency is lower than before, resulting in an increase in tank pressure during this period and a decrease in system performance. When C2 and C3 are repaired to a safe state, the processing efficiency of the BOG returns to the initial value, and the pressure in the tank gradually returns to the expected value. The expression of the system performance curve $P_2(t)$ under this scenario is obtained by using the fitting technique, as shown in Eq. (21). According to Eq. (10), the system resilience within 95 h is 0.664, as shown in Fig. 13.

$$P_2(t) = \begin{cases} 1.00074 - 0.02624 \cdot t + 2.01791 \times 10^{-4} \cdot t^2, 0 \le t < 34.3\text{h} \\ -0.39269 + 0.02531 \cdot t - 1.12636 \times 10^{-4} \cdot t^2, 34.3 \le t < 95\text{h} \end{cases} \tag{21}$$

Scenario 3: Severe disruption (the whole compressor system failure).

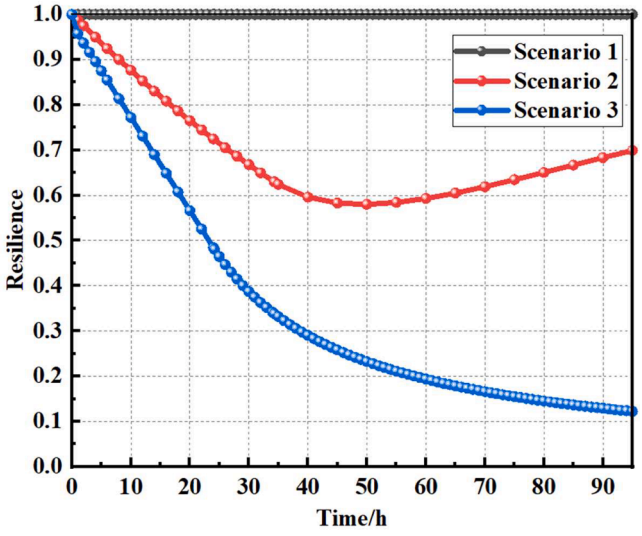

Fig. 13. System resilience in different disruption events.

When the compressor system is faulty, BOG accumulates in the storage tank. If the flare system and safety valve fail to work, the LNG tank pressure reaches the maximum operating pressure in 24.17 h, and the

system performance decreases to 0. Fig. 12(*b*) shows the performance response curve of this scenario. In order to accurately quantify the system resilience, the mathematical expression of the performance response curve was obtained by using data fitting technology, as shown in Eq. (22). On this basis, Eq. (10) is applied to quantify the system resilience, as shown in Fig. 13:

$$P_3(t) = \begin{cases} 0.97812 - 0.04118t, 0 \le t \le 24.17\text{h} \\ 0, 24.17 \le t \le 95\text{h} \end{cases} \quad (22)$$

As can be seen from Figs. 11–13, when C2 compressor fails, the redundant structure of the system can fully absorb the disruption, so that the performance of the system is not affected by the disruptive event (Scenario 1). When C2 and C3 fail simultaneously (Scenario 2), the absorption capacity of the system can partially absorb the impact caused by the disruption, so that the system can continue to run, and the residual effects of the disruption need to be dealt with through adaptation and restoration. When the entire compressor system fails (Scenario 3), the intensity of the disruptive event exceeds the absorption capacity of the system, leading to the pressure in the tank rising rapidly in a short time. As a result, the system performance declines rapidly, and if the safety valve and flare system fail to work, it will cause a serious accident. Those three different scenarios provide insights into the system's thresholds and the effectiveness of different resilience-enhancing strategies under severe stress conditions. Good resilience is characterized by minimal performance degradation following disruptions and a rapid return to a new equilibrium state. Essentially, a highly resilient system experiences less fluctuation in performance during disruptive events.

The intensity of different disruptive events is different, leading to various impact degrees on the system performance. The absorption capacity of the system can reduce the impact of disruptions on the system performance. When the disruption intensity is within the processing range of the system absorption capacity, the absorption capacity can fully or partially resist the influence of the disruptive event, reduce the performance loss of the system, and thus reduce the dependence of the system on the adaptation and restoration capacity. The absorption capacity of the system is dependent on the system structure. The absorption capacity of the system will change with the structure of the system. System structures can be optimized to improve the system's ability to cope with disruptive events, so as to improve the resilience of the system and ensure the system safety and production continuity.

When the disruption intensity is too large, the disruption will cause serious impact on the system performance, and even make the whole system fail. In this case of serious disruption, absorption and adaptation capacity have little impact on the system resilience. For example, in scenario 3, the compressor system fails, and the BOG in the LNG tank cannot be handled in time, resulting in increasing pressure in the tank. If the safety valve and flare system also fail, it may lead to the occurrence of overpressure accidents in the tank. In this situation, the system resilience depends on the restoration capacity of the system. The stronger the restoration capacity, the faster the failed compressor can be restored to the safe state, so as to timely deal with the BOG and prevent the occurrence of overpressure accidents.

It is worth noting that although the disruptive events are equipment failures, there are also human and organizational factors involved in how to adapt and recover from the failure state to normal operation after disruptions. For example, the emergency response time and repair rate are dependent on human and organizational factors. With good training and timely emergency response, the system can quickly recover from disruptions to new equilibrium state.

(2) Sensitivity analysis: Analysis of the influence of different restoration capacities on system resilience

Sensitivity analysis is an important step to verify the stability of the proposed methodology. Since scenario 3 has a large disruption intensity and a serious impact on the system, scenario 3 is selected to explore the effects of different absorption, adaptation and restoration capabilities on system performance and resilience. The system resilience is composed of absorption, adaptation and restoration capabilities, and the absorption capacity depends on the system structure. Since the resilience of the system under the different compressor failure combination scenarios in the LNG terminal system has been analyzed, as shown in Fig. 13, the influence of different absorption capacities on the system resilience will not be analyzed here.

Adaptation capacity determines the response time, and different response times determine the time from the moment of failure to the start of maintenance of the compressor. However, the maintenance time of the compressor is 30.30 h, whereas under the influence of scenario 3, the system performance drops to 0 in 24.17 h. Even if timely emergency response is carried out under scenario 3, the maintenance task is still unable to be completed before 24.17 h. Under this disruption, restoration capacity has the greatest impact on system resilience. Therefore, the effects of different restoration capacities on system performance and resilience are mainly explored here.

Under normal condition, the compressor repair rate μ is 0.076/h, and the time required to repair the faulty compressor to the safe state is 30.3 h. With the improvement of restoration capability, the compressor repair rate increases. The corresponding maintenance time for different repair rates is shown in Table 4.

Under the condition that the absorption and adaptation capacity of the system remain unchanged, the influence of different restoration capacities on tank pressure, system performance and resilience is explored by changing repair rate from 1 to 3 times. The results are shown in Figs. 14 and 15.

The influences of different restoration capabilities on tank pressure and system performance are shown in Fig. 14. It can be seen from Fig. 14, when the compressor repair rate is μ and 1.5μ, the total restoration time is 34.40 h and 24.20 h, respectively. The maintenance task cannot be completed before the maximum acceptable pressure inside the tank reaches 126 kPa. Under these two restoration capabilities, the system performance decreases to zero at 24.17 h. Based on Eq. (10), the system resilience is 0.127 under these two restoration capabilities. With the increase of restoration capability, the time for the failed compressor to recover to the safe state decreases. When the repair rate is 2μ, 2.5μ and 3μ, the time required for the compressor from fault occurrence to restart is 19.15 h, 16.12 h and 14.10 h, respectively. The failed compressor is brought back to safety in a timely manner from the disruptive event, so that the accumulated BOG in the tank can be dealt with and the tank overpressure can be prevented. With the restart of compressors, the tank pressure gradually decreases over time, as shown in Fig. 14.

The influence of varying restoration capacities on system resilience is graphically represented in Fig. 15. The value of resilience depicted in Fig. 15 represent a composite index of resilience, incorporating aspects such as absorption, adaptation and restoration capacities. Initially, with a system resilience of 0.127, attempts to enhance system restoration capacity through an increased repair rate of 1.5μ reveal minimal effective change in the system's performance curve. Consequently, the system resilience remains at 0.127 with this repair rate. However, as the repair rate of the compressor is progressively elevated, the system's resilience exhibits a corresponding increase. Notably, when the compressor repair rate reaches 2μ, 2.5μ, and 3μ, the system's resilience surges by factors of 2.93, 3.47, and 3.87, respectively. This underscores that augmenting the system's restoration capacity allows for more rapid recovery from disruptive events, ultimately ensuring the safety of system production.

Table 4
Compressor maintenance time corresponding to different repair rates.

Repair rate	μ	1.5μ	2μ	2.5μ	3μ
Repair time/h	30.30	20.20	15.15	12.12	10.10
Total restoration time/h	34.30	24.20	19.15	16.12	14.10

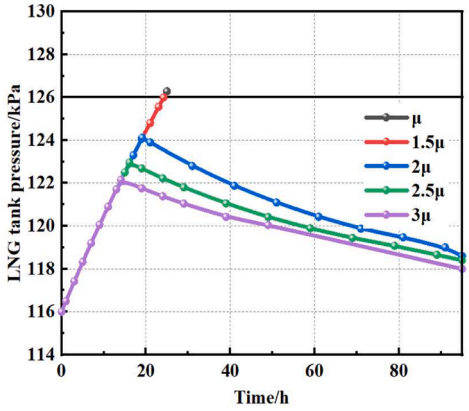

(*a*) The impact of different restoration capacities on tank pressure

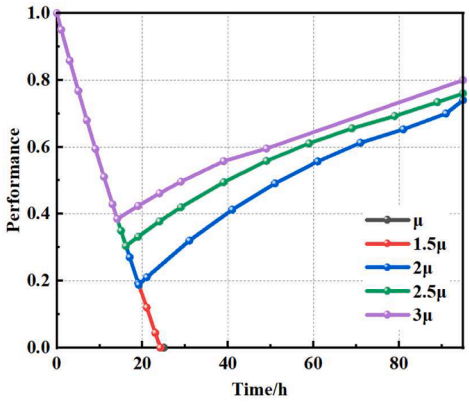

(*a*) The impact of different restoration capacities on system performance

Fig. 14. The influence of different restoration capacities on tank pressure (a) and system performance (b).

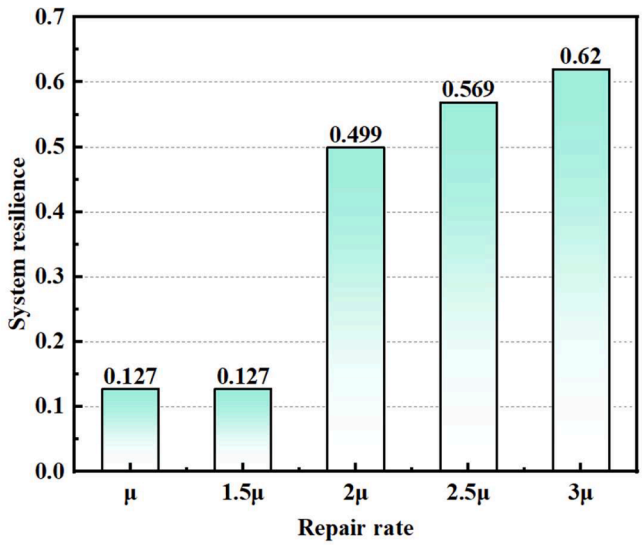

Fig. 15. The influence of different restoration capacities on system resilience.

4. Conclusions

Resilience should be a core consideration in the early stages of system design, enabling designers to harness this capacity to enhance the system's robustness. For established process systems, the path to bolstering resilience lies in a comprehensive assessment of the system's existing resilience.

This work proposed a methodology for resilience assessment of process systems. Towards the objective of evaluating and enhancing the resilience against abnormal events of process systems, the proposed methodology comprises four integral components: system structure analysis, analysis of disruption impacts, process simulation, and resilience assessment. Specifically, a process parameters-based performance indicator is introduced to reduce the data uncertainty. Simulations are conducted on a practical LNG terminal system to acquire time-dependent process parameters and to quantify the complex dynamic response mechanism of various parameters under the influence of disruptive events. The results show that the proposed methodology can not only reduce the data uncertainty, but also reflect the influence of disruptive events on the system explicitly. Furthermore, to improve system resilience under different types of disruptive events, targeted strategies (e.g., different redundancies, maintenance resources) are investigated and developed accordingly. Finally, sensitivity analysis is carried out to validate the proposed methodology.

In the realm of future research, a diverse array of internal factors (such as human elements, and external disruptions, including natural disasters and cyberattacks) will be investigated. This exploration aims to construct a comprehensive and systematic resilience assessment for process systems. By doing so, the safety of process systems under disruptive events can be enhanced. This endeavor not only advances the field but also offers a solid theoretical foundation for ensuring safe production and informed decision-making.

CRediT authorship contribution statement

Hao Sun: Writing – original draft, Methodology, Investigation, Funding acquisition, Formal analysis, Data curation, Conceptualization. **Ming Yang:** Writing – review & editing, Validation, Supervision. **Enrico Zio:** Writing – review & editing, Validation, Supervision. **Xinhong Li:** Writing – review & editing, Validation. **Xiaofei Lin:** Conceptualization. **Xinjie Huang:** Investigation. **Qun Wu:** Data curation.

Declaration of competing interest

The research being report in this paper titled "A simulation-based approach for resilience assessment of process system: A case of LNG terminal system" was supported by Anhui University of Technology and Delft University of Technology. The authors of this paper have the IP ownership related to the research being reported. The terms of this arrangement have been reviewed and approved by the university in accordance with its policy on objectivity in research.

Acknowledgments

The authors gratefully acknowledge the financial support provided by the Anhui University of Technology Young Teachers Research Fund Project (QZ202315) and Anhui University of Technology Introduction of Talent Research Start-up Fund (QD202368).

References

[1] Huang KX, Chen GH, Khan F, et al. Dynamic analysis for fire-induced domino effects in chemical process industries. Process Saf Environ Prot 2021;148:686–97.
[2] Abbassi R, Khan F, Garaniya V, Chai S, Chin C, Hossain K. An integrated method for human error probability assessment during the maintenance of offshore facilities. Process Saf Environ Prot 2015;94:172–9.
[3] Liu X, Wang C, Yin ZM, et al. Risk-informed multi-objective decision-making of emergency schemes optimization. Reliab Eng Syst Saf 2024;245:109979.

[4] Wang R, Nellippallil AB, Wang GX, et al. A process knowledge representation approach for decision support in design of complex engineered systems. Adv Eng Inform 2021;48:101257.
[5] Fang YP, Zio E. Unsupervised spectral clustering for hierarchical modelling and criticality analysis of complex networks. Reliab Eng Syst Saf 2013;116:64–74.
[6] Mühlhofer E, Koks E, Kropf C, et al. A generalized natural hazard risk modelling framework for infrastructure failure cascades. Reliab Eng Syst Saf 2023;234:109194.
[7] Li XH, Ma J, Pasman H, et al. Dynamic risk investigation of urban natural gas pipeline accidents using Stochastic Petri net approach. Process Saf Environ Prot 2023;178:933–46.
[8] Zio E. The future of risk assessment. Reliab Eng Syst Saf 2018;177:176–90.
[9] Meng HX, An X, Li DW, et al. A STAMP-Game model for accident analysis in oil and gas industry. Pet Sci 2023. https://doi.org/10.1016/j.petsci.2023.12.002.
[10] Sun H, Yang M, Wang H. Resilience-based approach to maintenance asset and operational cost planning. Process Saf Environ Prot 2022;162:987–97.
[11] Marino A, Zio E. A framework for the resilience analysis of complex natural gas pipeline networks from a cyber-physical system perspective. Comput Ind Eng 2021;162:107727.
[12] Chen C, Yang M, Reniers G. A dynamic stochastic methodology for quantifying HAZMAT storage resilience. Reliab Eng Syst Saf 2021;215:107909.
[13] Hosseini S, Barker K, Ramirez-Marquez JE. A review of definitions and measures of system resilience. Reliab Eng Syst Saf 2016;145:47–61.
[14] Sun H, Yang M, Wang H. A virtual experiment for measuring system resilience: a case of chemical process systems. Reliab Eng Syst Saf 2022;228:108829.
[15] Yang M, Sun H, Geng SY. On the quantitative resilience assessment of complex engineered systems. Process Saf Environ Prot 2023;174:941–50.
[16] Kottmann F, Kyriakidis M, Sansavini G, et al. A human operator model for simulation-based resilience assessment of power grid restoration operations. Reliab Eng Syst Saf 2023;238:109450.
[17] Holling CS. Resilience and stability of ecological systems. Annu Rev Ecol Evol Syst 1973;4:1–23.
[18] Darling KA, Kale C, Turnage S, et al. Nanocrystalline material with anomalous modulus of resilience and springback effect. Scr Mater 2017;141:36–40.
[19] Jain P, Rogers WJ, Pasman H, et al. A Resilience-based Integrated Process Systems Hazard Analysis (RIPSHA) approach: part I plant system layer. Process Saf Environ Prot 2018;148:92–105.
[20] Amer L, Erkoc M, Celik N, et al. Operationalizing resilience: a deductive fault-driven resilience index for enabling adaptation. Process Saf Environ Prot 2023;177:1085–102.
[21] Chen C, Li J, Zhao YX, et al. Resilience assessment and management: a review on contributions on process safety and environmental protection. Process Saf Environ Prot 2023;170:1039–51.
[22] Tong Q, Gernay T. Resilience assessment of process industry facilities using dynamic Bayesian networks. Process Saf Environ Prot 2023;169:547–63.
[23] Haimes YY. On the definition of resilience in systems. Risk Anal 2009;29(4):498–501.
[24] Francis R, Bekera B. A metric and frameworks for resilience analysis of engineered and infrastructure systems. Reliab Eng Syst Saf 2014;121:90–103.
[25] Cottam B, Specking EA, Small CA, et al. Defining resilience for engineered systems. Eng Manag Res 2019;8(2):11–29.
[26] Fang YP, Zio E. An adaptive robust framework for the optimization of the resilience of interdependent infrastructures under natural hazards. Eur J Oper Res 2019;276:1119–36.
[27] Sun H, Wang H, Yang M, et al. Resilience-based approach to safety barrier performance assessment in process systems. J Loss Prev Process Ind 2021;73:104599.
[28] An X, Yin ZM, Tong Q, et al. An integrated resilience assessment methodology for emergency response systems based on multi-stage STAMP and dynamic Bayesian networks. Reliab Eng Syst Saf 2023;238:109445.
[29] Kammouh O, Gardoni P, Cimellaro GP. Probabilistic framework to evaluate the resilience of engineering systems using Bayesian and dynamic Bayesian networks. Reliab Eng Syst Saf 2020;198:106813.
[30] Cai BP, Zhang YP, Wang HF, et al. Resilience evaluation methodology of engineering systems with dynamic-Bayesian-network-based degradation and maintenance. Reliab Eng Syst Saf 2021;209:107464.
[31] Zinetullina A, Yang M, Khakzad N, et al. Quantitative resilience assessment of chemical process systems using functional resonance analysis method and dynamic Bayesian network. Reliab Eng Syst Saf 2021;205:107232.
[32] Iannacone L, Sharma N, Tabandeh A, et al. Modeling time-varying reliability and resilience of deteriorating infrastructure. Reliab Eng Syst Saf 2022;217:108074.
[33] Orosz A, Pimentel J, Argoti A, et al. General formulation of resilience for designing process networks. Comput Chem Eng 2022;165:107932.
[34] Dui HY, Lu YH, Gao ZF, Xing LD. Performance efficiency and cost analysis of multi-state systems with successive damage and maintenance in multiple shock events. Reliab Eng Syst Saf 2023;238:109403.
[35] Zeng Z, Fang Y, Zhai Q, Du S. A Markov reward process-based framework for resilience analysis of multistate energy systems under the threat of extreme events. Reliab Eng Syst Saf 2021;209:107443.
[36] Zhu CL, Qi M, Jiang JC. Quantifying human error probability in independent protection layers for a batch reactor system using dynamic simulations. Process Saf Environ Prot 2020;133:243–58.
[37] Cui CT, Qi M, Shu CM, Liu Y. Rigorous dynamic simulation methodology for scenario-based safety analysis of pressure-swing distillation considering independent protections. Process Saf Environ Prot 2023;172:282–304.
[38] Yandrapu VP, Kanidarapu NR. Process design for energy efficient, economically feasible, environmentally safe methyl chloride production process plant: chlorination of methane route. Process Saf Environ Prot 2021;154:360–71.
[39] Bruneau M, Chang SE, Eguchi RT, et al. A framework to quantitatively assess and enhance the seismic resilience of communities. Earthq Spectra 2003;19:733–52.
[40] Pawar B, Huffman M, Khan F, Wang QS. Resilience assessment framework for fast response process systems. Process Saf Environ Prot 2022;163:82–93.
[41] Pramoth R, Sudha S, Kalaiselvam S. Resilience-based Integrated Process System Hazard Analysis (RIPSHA) approach: application to a chemical storage area in an edible oil refinery. Process Saf Environ Prot 2020;141:246–58.
[42] Pasman H, Kottawar K, Jian P. Resilience of process plant: what, why, and how resilience can improve safety and sustainability. Sustainability 2020;12:6152.
[43] Patriarca R, Paolis AD, Costantino F, et al. Simulation model for simple yet robust resilience assessment metrics for engineered systems. Reliab Eng Syst Saf 2021;209:107467.
[44] Bellegoni M, Chicchiero C, Landucci G, et al. A UQ based calibration for the CFD modeling of the gas dispersion from an LNG pool. Process Saf Environ Prot 2022;162:1043–56.
[45] Iannaccone T, Scarponi GE, Landucci G, et al. Numerical simulation of LNG tanks exposed to fire. Process Saf Environ Prot 2021;149:735–49.
[46] Hu JQ, Dong SH, Zhang LB, et al. Cyber-physical-social hazard analysis for LNG port terminal system based on interdependent network theory. Saf Sci 2021;137:105180.
[47] Landucci G, Argenti F, Cozzani V, Reniers G. Assessment of attack likelihood to support security risk assessment studies for chemical facilities. Process Saf Environ Prot 2017;110:102–14.
[48] OREDA, 2002. Offshore reliability data handbook. DNV, Trondheim, Norway.
[49] Chang YJ, Wu XF, Zhang CS, et al. Dynamic Bayesian networks based approach for risk analysis of subsea wellhead fatigue failure during service life. Reliab Eng Syst Saf 2019;188:454–62.